Article

Electrochemical Reduction of Pd-Nd$_2$O$_3$-CeO$_2$ Mixtures in the LiCl-Li$_2$O Melt

Alexey V. Shishkin *, Vladimir Yu. Shishkin, Anna A. Maslennikova [ID], Aleksander B. Salyulev, Peter N. Mushnikov [ID] and Yury P. Zaikov [ID]

Institute of High Temperature Electrochemistry, Ural Branch of the Russian Academy of Sciences, 20 Akademicheskaya Str., 620990 Ekaterinburg, Russia
* Correspondence: a.v.shishkin81@mail.ru

Abstract: The electrochemical reduction of pelleted heterophase powder Pd-Nd$_2$O$_3$-CeO$_2$ mixtures was studied in molten LiCl-Li$_2$O (1–1.5 wt%) at 650 °C. The influence of the composition of the mixture, as well as electrochemical factors—i.e., the amount of electricity passed and the cathode potential during electrolysis—were considered. It was found that in the presence of metallic palladium, neodymium and cerium oxides are reduced by lithium released at the cathode and form intermetallic compounds of different compositions. At potentials more positive than the formation of a phase based on liquid lithium at 0.5–0.8 V, CePd$_3$ and NdPd$_3$ intermetallic compounds are present in the reduced product. At potentials close to the formation of liquid lithium, a whole spectrum of intermetallic compounds is synthesized: CePd, NdPd, Ce$_3$Pd$_4$, and Nd$_3$Pd$_4$. The mechanisms of formation of palladium alloys with neodymium and cerium are proposed and considered. The degree of the reduction of lanthanide oxides was calculated from the data on the concentration of residual oxygen in the reduced product.

Keywords: metallization; spent nuclear fuel; rare earth metal oxide; reduction; intermetallic compounds

1. Introduction

The "metallization" of spent nuclear fuel (SNF) from uranium and plutonium oxides is complicated by the simultaneous presence of fission fragments, primarily rare-earth oxides and noble metals of the platinum group, such as palladium, ruthenium, and rhodium [1,2]. In previous studies, we have shown that uranium dioxide is almost completely reduced by lithium in a molten mixture of its chloride with a low oxide content—the degree of metal product yield in the process is high [3]—while the reduction of pure rare earth metal (REM) oxides (La$_2$O$_3$, Nd$_2$O$_3$, CeO$_2$) demonstrated negative results [4]. Such behavior of rare earth metal (REM) oxides should result in their concentration in the slag phase at the cathode product remelting. However, during the electrochemical reduction process, the simultaneous presence of lanthanide oxides and elements of the platinum group in the mixed nuclear fuel can lead to the formation of a metal phase in the form of intermetallic compounds [5–8] consisting of lanthanides and palladium, rhodium, and ruthenium. These elements will concentrate in the metallic phase alongside uranium and plutonium. Therefore, this fact provokes additional difficulties in separating the target components (U and Pu) from lanthanides (Ln, Pd, Ru, Rh) during the further processing of the metallized cathode product during the electrochemical refining in the eutectic LiCl-KCl melt, i.e., processing of metallic SNF [9,10]. That is why it is essential to analyze the conditions of REM and platinum metals alloys' formation processes during the electrolysis of the LiCl-Li$_2$O melt and to compare them with the corresponding values of the reactions with actinide metals. Hence, the optimal parameters of reduction electrolysis may be determined considering the separate reduction of the alloy components.

However, there is a lack of literature data where the presence of REM and noble metals intermetallic compounds is discussed. The present research is focused on the experimen-

tal study of the electrochemical reduction of Pd-Nd_2O_3-CeO_2 oxide. The conditions of intermetallic compounds' formation are analyzed.

The purpose of this work is to evaluate the possibility of reducing REM oxides (Nd_2O_3, CeO_2) and noble metals (Pd) containing pellets, located on the cathode, by lithium during the electrolysis of the LiCl-Li_2O (1.5 wt%) melt at different cathode potentials: positive 0.5–0.8 V relative to Li^+/Li^0 and potentials close to or equal to the potential of a liquid lithium-based phase formation.

2. Materials and Methods

2.1. Preparation of Reagents

We used commercial chemically pure anhydrous lithium chloride with the content of the main component of 99.3 wt%. To remove residual moisture, the salt was evacuated with gradual heating and melted in an argon atmosphere. To remove the remaining oxygen impurities, the zone melting method was used; the process was performed in a nickel boat under an argon flow purified from traces of oxygen and water vapor [11,12]. Commercial chemically pure lithium oxide contained at least 99.5 wt% of the main component. It was examined for the content of moisture, hydroxide, and lithium carbonate by infrared spectroscopy using FTIR TENSOR 27 (Bruker, Mannheim Germany), the total content of which did not exceed 0.05 wt%. Pellets composed of a mixture of Nd_2O_3 and CeO_2 oxide powders (99% purity, Alfa Aesar, UK) and powder of metallic palladium (high purity 99.9%) had a porosity of 20–25% and the following dimensions: height 2–3 and diameter 10.1–10.2 mm. They were prepared by pressing powders with a fraction of 5–50 μm using a commercial zinc stearate of a technical grade (Aldrich, Saint Louis, MO, USA) as a binding agent under a pressure of 370–650 MPa, followed by annealing in air with gradual heating at a rate of 150–200 °C per hour to a temperature of 1100 °C and 2-h exposure. Pellets of the following compositions were synthesized according to the weight: Pd:Nd_2O_3 = 1:1, Pd:CeO_2 = 1:1, Pd:Nd_2O_3:CeO_2 = 1:1:1, Pd:Nd_2O_3:CeO_2 = 1:0.5:0.5.

2.2. Process Parameters

Electrolysis was carried out in an electrolytic cell, described in detail in our previous works [3,4]. The process temperature was 650 °C. A quartz glass (50 cm high and 9 cm in diameter) served as a device case. A metal (nickel) container was placed at the bottom of the glass. A total of 300 g of the LiCl-Li_2O (~1.5 wt%) mixture was loaded into the Ni container. The anode assembly consisted of a rod made of high-density lithium oxide doped nickel oxide ceramics, which was placed in a zirconium oxide doped magnesium oxide ceramic sheath. The anode was partially immersed into the electrolyte, and a platinum wire with a diameter of 1.0 mm served as a current lead. A basket woven from stainless wire with two pellets of REM oxide with palladium served as a cathode. To carry out electrochemical measurements and, first of all, to determine the potential of the cathode and anode during the electrolysis and other manipulations, a reference electrode made of Bi-Li alloy (60 mol%) was used. The reference electrode was prepared directly in the electrolytic cell prior to the electrochemical studies on the reduction of REM oxides. To determine the potential value of the resulting alloy relative to the lithium extraction potential, an auxiliary electrode made of molybdenum wire with a diameter of 1–1.5 mm and a surface area of 0.3–0.5 cm^2 was used. The auxiliary electrode was immersed into the salt melt. The voltammetry curves were recorded. When the molybdenum electrode was used as the working electrode, the anode served as the auxiliary electrode, and bismuth was used as the reference electrode. The reference electrode was calibrated according to the lithium extraction potential. All structural components of the cell were hermetically attached to a cover using seals made of vacuum-tight silicone rubber, and the cover itself with all technological openings and details was made of fluoroplastic.

All operations for assembling the cell manipulations with LiCl-Li_2O were carried out in a glove box in an argon atmosphere with the oxygen content not exceeding 10 ppm and water vapor of 0.1 ppm.

The electrolysis was carried out in the galvanostatic mode, the necessary process parameters were set and controlled using a PGSTAT AutoLab device (Ecohemie, Utrecht, The Netherlands). The anode potential was controlled using a universal digital voltmeter GM Instek GDM-78351 (GW Instek, Taiwan, China). During the experiment, the electrolyte samples were taken, and the current content of lithium oxide was determined by the acid-base titration. The chemical analysis of the solutions was carried out using an optical emission spectrometer with inductively coupled plasma Optima 4300 DV (Perkin Elmer, Waltham, MA, USA). The degree of reduction of oxides was calculated using the data on the residual oxygen content in the reduced product after removal of the electrolyte by vacuum distillation [13]. To determine the oxygen concentration, a METAVAK-AK device (Eksan, Saratov, Russia) was used. The presence of phases of rare earth alloys with palladium, as well as that of lanthanide oxides, was determined in the reduced sample using X-ray phase analysis on an automatic diffractometer Rigaku 600 (Rigaku, Tokyo, Japan).

3. Results

Intermetallic compounds of uranium and palladium form highly strong compounds; therefore, the potentials of their formation shift to the more positive region. It is important to determine the region of uranium-containing intermetallic compounds, to correlate them with the analogous data for lanthanide oxides, and to analyze the influence of the solubility of the corresponding oxides on the intermetallic compounds' reduction and formation processes.

In the present work, we performed six experimental runs, which are divided into two series.

1. The electrolysis was carried out in the galvanostatic mode following the algorithm; electrolysis was performed during 600 s and then it was interrupted for 60 s to measure the potentials of the cathode and anode. During the measurements, the current was turned off. The cathode potential was maintained at ~0.8 V, more positive than the potential for the formation of a liquid phase based on lithium. Over time, the cathode potential shifted to the negative side; in order to maintain it at a given value, the current was reduced. Thus, a stepwise galvanostatic mode of electrolysis was realized;
2. Another series of experiments, in contrast to the first one, was carried out at potentials close to the potential for the lithium-based liquid phase formation.

Table 1 illustrates the main parameters for the electrochemical reduction of pelleted samples consisting of palladium and REM oxide powders. Table 2 presents the main experimentally obtained results of electrochemical reduction.

The chosen lanthanide oxides were found to reduce with the formation of metallic phase, which is the palladium-containing intermetallic compound, in wide range of cathode potentials. The composition of alloys changes correspondingly as the reduction potentials shift to the region of alkali metal based liquid phase formation. The intermetallic compounds form at the cathode at positive potentials.

Table 1. Electrochemical reduction parameters.

Run nº	Pellets (Amount)	Composition	Wt., g	Q_{exp}/Q_{theor} %	$E_{cathode}$; Q%	Current, A
1	2	$Nd_2O_3 + Pd = 1{:}1$	1.066	125	$0.78 \div 0.88$ V; 100%	$0.4 \div 0.6$
2	2	$CeO_2 + Pd = 1{:}1$	1.073	357	$0.80 \div 0.90$ V; 72%	$0.6 \div 1.2$
3	2	$CeO_2 + Pd = 1{:}1$	0.430	168	$0.03 \div 0.190$ V; 28%	0.8
		$Nd_2O_3 + Pd = 1{:}1$	0.689	168	$0.78 \div 0.040$ V; 100%	0.8

Table 1. *Cont.*

Run n°	Pellets (Amount)	Composition	Wt., g	Q_{exp}/Q_{theor} %	$E_{cathode}$; Q%	Current, A
4	2	$Pd + Nd_2O_3 + CeO_2 = 1:1:1$	1.49	172	0.003 V; 100%	0.8 ÷ 0.2
5	2	$Pd + Nd_2O_3 + CeO_2 = 1:0.5:0.5$	2.01	186	0.9 V; 14.7% 0.2 ÷ 0.006 V; 85.3%	0.1 ÷ 0.7 1.0 ÷ 0.5
6	2	$Pd + Nd_2O_3 + CeO_2 = 1:0.5:0.5$	2.10	247	0.9 V; 22% 0.2 ÷ 0.006 V; 78%	0.1 ÷ 0.7 1.0 ÷ 0.5

Table 2. Characterization of samples after reduction.

Run n°	Amount of Electrolyte Captured by the Pellet, wt%	$[Li_2O]$, wt% LiCl	[O], wt%	Reduction Degree, β%	Basic Phases	Recorded	[Ln] Alloy, at. %
1	17	1.54	4.50	42.2	$LiCl, NdPd_3, Nd_2O_3$	$LiNdO_2$	21.1
2	17	1.54	3.04	61.1	$LiCl, CePd_3, Ce_2O_3$	$CeOCl, Li_2O$	27.5
3	17	1.52	3.40	56.16	$LiCl, CePd_3$	$LiCeO_2, Li_2O$	25.8
		1.54	3.44	55.5	$NdPd_3, Nd_3Pd_4$	$LiNdO_2, Nd_2O_3$	26.0
4	19.5	1.52	4.57	55.3	$LiCl, NdPd,$ $CePd,$ $Nd_2O_3,$ Ce_2O_3		41
5	16.5	1.50	2.51	68.5	$LiCl, Nd_3Pd_4,$ Ce_3Pd_4	$Nd_7Pd_3, LiPd$	49.2
	16.5	1.5	3.01	61.6			47.5
6	16.8	1.46	0.59	95.4	After ethanol rinsing: $Nd_3Pd_4,$ Ce_3Pd_4		54.3

3.1. Run 1

Two pellets of the same composition were placed into the cathode basket. Figure 1 illustrates the pellets and the cathode basket before and after the experiment.

The initial calculated porosity of the pellets was ~20–25%. The electrolysis was carried out at a cathode potential of 0.78–0.88 V relative to Li^+/Li^0. After the completion of the process, the basket with pellets was lifted from the molten salt electrolyte, kept for some time above the surface for the melt to drain, and removed from the electrolytic cell for further manipulation. The pellets were visually examined and broken into pieces. The electrolyte captured by the samples was removed, depending on the purpose of the further studies, either by rinsing in dehydrated ethanol or by vacuum distillation [13]. All manipulations with the reduced samples were carried out in a glove box in the argon atmosphere. After electrolysis, the shape and size of the pellets remained almost unchanged. Tables 1 and 2 show all main parameters of the process, as well as the characteristics of the recovered samples. A part of the sample was ground in an agate mortar and examined on a Rigaku diffractometer in a special sealed cuvette with an inert atmosphere. Some of the pellets were evacuated in order to distill the trapped electrolyte for further analysis on METAVAK-AK to determine the residual oxygen content. The oxygen content in the sample was found primarily in the unreduced neodymium or cerium oxide and the lithium oxide remaining after distillation. The amount of lithium oxide in the sample was determined based on its content in the electrolyte at the end of the electrolysis and the mass of electrolyte captured by the porous pellet. The degree of REM oxide reduction to metal (β) was defined

as the ratio of reduced metal ($m_{Ln(Pd)}$) to the mass of the total lanthanide metal (m_{Ln}) in the sample:

$$\beta(\%) = 100 \times m_{Ln(Pd)}/m_{Ln.}$$

Data on the oxygen content in the sample associated with lithium oxide allow us to calculate the degree of reduction and, consequently, the amount of reduced metal. Thus, based on the fact that palladium was detected only in an alloy with neodymium or cerium in the X-ray diffraction pattern of the sample, and the independent phase of palladium was not detected, it is possible to calculate the concentration of lanthanide in the alloy with palladium with a known approximation. The X-ray diffraction pattern of the sample reduced in this experiment is illustrated in Figure 2. The main phases are $NdPd_3$, Nd_2O_3, and LiCl. The $LiNdO_2$ phase is also confidently fixed. A shift in the position of the characteristic diffraction maxima of the $NdPd_3$ intermetallic compound was recorded towards larger angles compared to the tabular data for the stoichiometric compound, which is associated with a decrease in the cubic lattice parameter due to an increase in the palladium concentration compared to the stoichiometric value. The calculated concentration of neodymium in the intermetallic compound was 21.1 at.%.
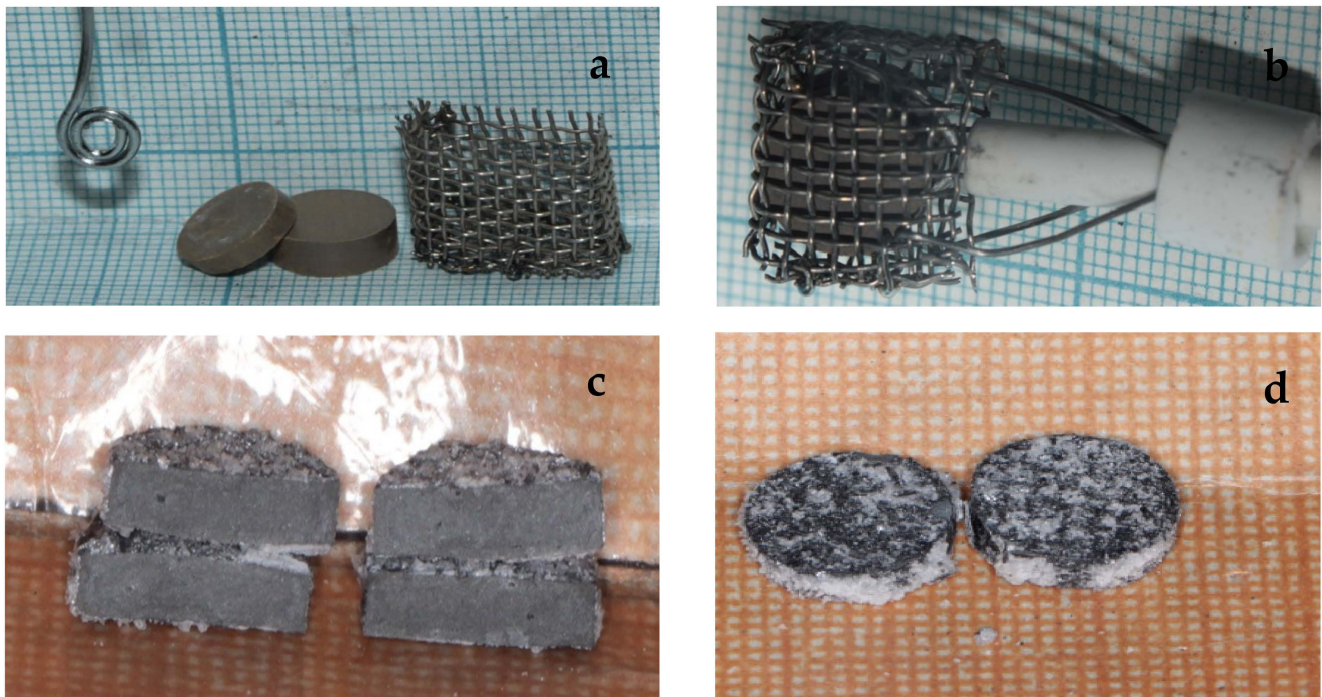

Figure 1. Appearance of experimental samples (pellets) before (**a**,**b**) and after (**c**,**d**) the reduction process and the pellets cross section after the reduction (**c**).
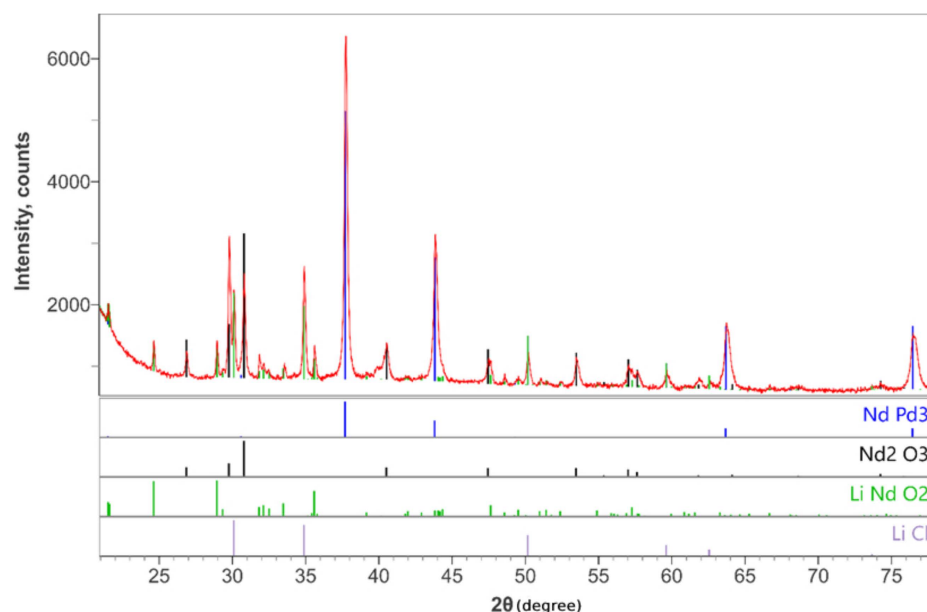
Figure 2. X-ray pattern of the Pd:Nd$_2$O$_3$ = 1:1 sample, reduced at positive potentials without removing the trapped electrolyte (Run 1), Q$_{exp}$/Q$_{theor}$ = 125%, β = 42.2%. Red line denotes the contour of the experimentally obtained X-ray pattern.

3.2. Run 2

The experiment was carried out with pellets containing cerium dioxide. A significantly larger amount of electricity was passed in relation to the theoretical value necessary for the CeO$_2$ reduction by lithium to metal: Q$_{exp}$/Q$_{theor}$ = 357%. At cathode potentials of 0.80–0.90 V relative to Li$^+$/Li^0, 78% of the total amount of electricity (coulomb) was passed, and at the end of electrolysis, the potential gradually changed from 0.19 to 0.03 V. The powder diffraction pattern of the reconstituted pellets is presented in Figure 3. The main phases are CePd$_3$, Ce$_2$O$_3$, and LiCl. The CeOCl phase is confidently fixed. Two cubic phases of CePd$_3$ were recorded with different lattice parameters [14]: one with parameters close to the tabular data corresponding to the stoichiometric composition of the alloy; and another one with a significantly larger lattice parameter; its reflections in the diffraction pattern are significantly shifted towards smaller angles. This means that the concentration of cerium in the alloy is higher than the stoichiometric one. The calculated average concentration of cerium in the intermetallic compound is 27.5 at.%. The calculations are based on data on the oxygen concentration in the reduced sample after distillation, taking into account lithium oxide remaining in the sample and the fact that all palladium is bound to neodymium in the intermetallic compound. Judging by the intensity of the lines on the diffraction pattern, the phase with an increased lattice parameter is much less than from the phase close to the stoichiometric composition, which, most likely, is formed at potentials of 0.80–0.90 V relative to Li$^+$/Li^0. Changing the potential to values of 0.19 and then to 0.03 V results in a sharp increase in the activity of lithium in the system and creates conditions for an additional reduction of cerium at the surface of the already-existing intermetallic compound, which, in turn, leads to the formation of a phase with a high REM content. Thus, a part of the phase close to stoichiometric is converted into an alloy with a high content of cerium.
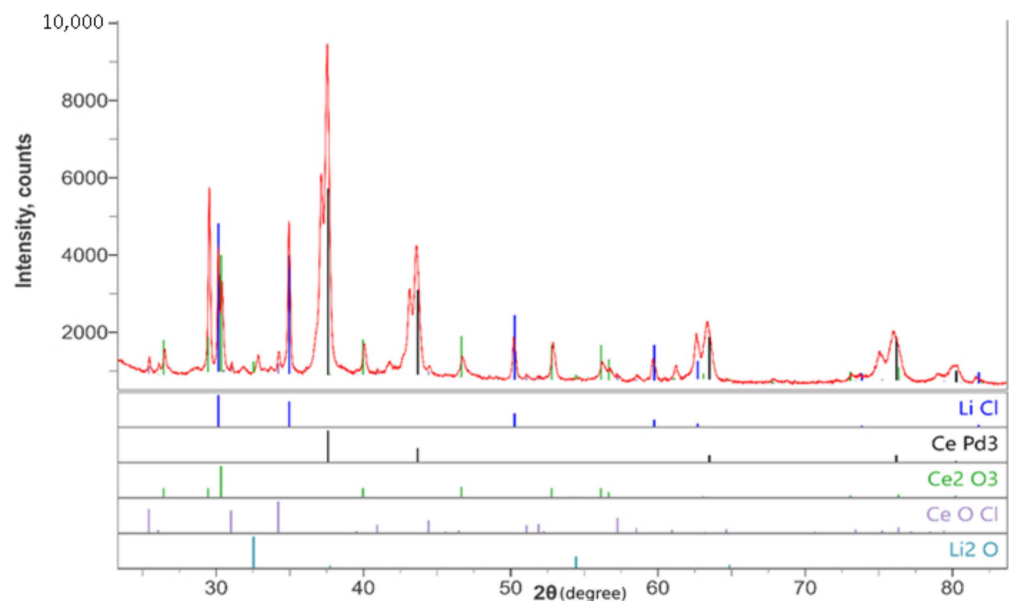
Figure 3. X-ray pattern of the Pd:CeO$_2$ = 1:1 sample reduced at positive potentials without removing the trapped electrolyte (Run 2), Q$_{exp}$/Q$_{theor}$ = 125%, β = 42.2%.

3.3. Run 3

Two pellets composed of CeO$_2$ + Pd and Nd$_2$O$_3$ + Pd powders were used in the experiment; the ratio of oxide to palladium was 1:1. A distinctive feature of this experiment is that the value of the potential changed monotonously from 0.78 to 0.040 V. For both pellets, X-ray diffraction patterns show reflections corresponding to LnPd$_3$ phases, but they are significantly shifted towards smaller angles, which indicates an increase in the cubic lattice parameter as a result of an increase in the lanthanide concentration compared to stoichiometry. Apparently, this is a consequence of an increase in the activity of the alkali metal in the reduction process, which creates conditions for obtaining alloys with a higher activity of lanthanide. The presence of LiCeO$_2$ and LiNdO$_2$ phases should be noted.

3.4. Run 4

In this experiment, the ratio of palladium and REM oxides was significantly changed (Pd:Nd$_2$O$_3$:CeO$_2$ = 1:1:1). In addition, the reduction was carried out at potentials practically equal to the alkali metal-based liquid-phase formation during the entire electrolysis. The diffraction pattern of the reduced sample (Figure 4) reflects the existence of NdPd and CePd in addition to LiCl, Ce$_2$O$_3$, and Nd$_2$O$_3$. Thus, an increase in the activity of lithium almost to that of pure alkali metal makes it possible to form alloys of lanthanides with palladium, where the activity of neodymium or cerium is much higher than in previous cases. The average calculated content of lanthanide in palladium is ~41%.

3.5. Run 5

The ratio of components in the pellet is Pd:Nd$_2$O$_3$:CeO$_2$ = 1:0.5:0.5. At the beginning of the electrolysis, the potential at the cathode was ~0.9 V relative to Li$^+$/Li^0, and approximately 14.7% of the total amount of electricity was passed through the melt. The rest of the time, the potential changed monotonously from 0.2 to 0.006 V. The total amount of electricity passed through the melt Q$_{exp}$/Q$_{theor}$ = 186%. The main phases in the samples: LiCl, Nd$_3$Pd$_4$, Ce$_3$Pd$_4$. The calculated content of lanthanide in the alloy with palladium is ~49.2% for neodymium and 47.2% for cerium.
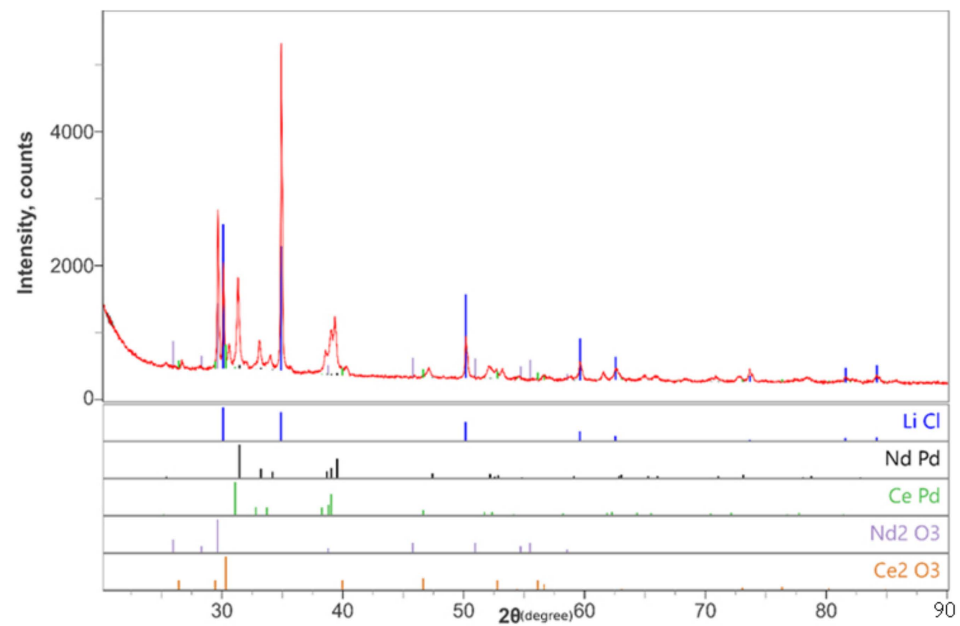
Figure 4. X-ray pattern of a Pd:Nd_2O_3:CeO_2 = 1:1:1 pellet reduced at negative potentials (Run 4), Q_{exp}/Q_{theor} = 172%, β = 55.3.

3.6. Run 6

The composition of the pellet was Pd:Nd_2O_3:CeO_2 = 1:0.5:0.5. At a cathode potential of ~0.9 V relative to Li+/Li0, Q = 22% of the total amount of electricity passed; at a potential of 0.2 to 0.006 V, 78% was missed. The total amount of the electricity passed was Q_{exp}/Q_{theor} = 247%. After washing the reduced samples in ethanol, the following phases were identified: Nd_3Pd_4 and Ce_3Pd_4. Figure 5 illustrates the X-ray pattern of the Pd:Nd_2O_3:CeO_2 sample.
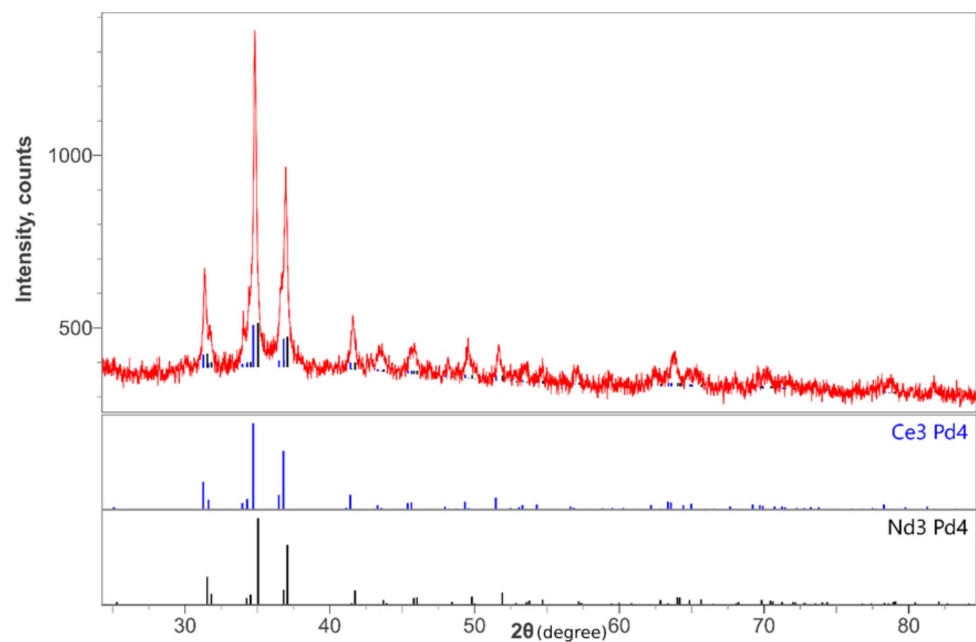

Figure 5. X-ray pattern of the Pd:CeO_2:Nd_2O_3 = 1:0.5:0.5 sample reduced at negative potentials and rinsed in ethanol (Run 6), Q_{exp}/Q_{theor} = 247%, β = 95.5%.

4. Discussion

Electrolysis at positive cathode potentials leads to the formation of $NdPd_3$ and $CePd_3$ intermetallic phases in the reduced samples. It is also important to note the fixed phases: $LiNdO_2$ and $CeOCl$. The absence of a metallic palladium phase apparently indicates that all palladium is bound to intermetallic compounds with neodymium and cerium. The absence of the initial CeO_2 phase and, conversely, the appearance of Ce_2O_3 phase indicates the almost complete reaction:
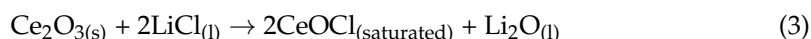
$$2CeO_2 + 2Li \rightarrow Ce_2O_3 + Li_2O. \tag{1}$$
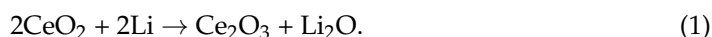
In the samples reduced at negative potentials, the expected phases are reliably fixed: lithium chloride, REM oxides. In addition, there are intermetallic compounds of palladium with cerium and neodymium. The REM content in the formed intermetallic compounds is greater—$NdPd$, $CePd$, Nd_3Pd_4, Ce_7Pd_3—which is illustrated in Figures 4 and 5. In this case, apparently, the formation of low-melting alloys of lithium with palladium (with a melting point below 923 K) is likely to play a (decisive) role in the formation of alloys. The formation of liquid alloys of palladium and lithium with an alkali metal content significantly higher than 60 at.% correspond to the cathode potentials close to the formation of a phase based on liquid lithium in equilibrium. Therefore, the process of REM oxide reduction is provided by the contact of a liquid alloy (Pd-Li) [15,16] with solid Nd_2O_3 and Ce_2O_3 particles, resulting in a reaction that, for example, for neodymium, can be presented as:

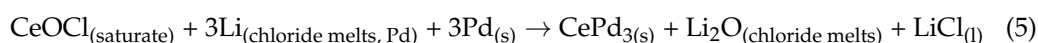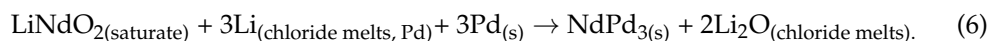$$Nd_2O_{3(s)} + 6Li_{(Pd)(l)} + 2Pd_{(Li)(l)} \rightarrow 3Li_2O_{(chloride\ melts)} + 2NdPd_{(s).} \tag{2}$$
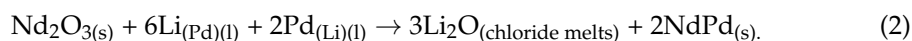
The process is affected greatly by a significant initial porosity of the pelleted samples (~25%), which contributes to the impregnation of the sample with a salt melt that ensures the transport of lithium ions to palladium outside and inside the pellet, followed by the subsequent release of atomic lithium and the formation of a palladium alloy with the required concentration of alkali metal. The fact that the salt melt is a collector of the resulting lithium oxide is equally important [17,18].

Obviously, when the reduction process is carried out at significantly more positive potentials with respect to the formation of liquid lithium, the concentration of alkali metal in palladium is not sufficient to form a liquid alloy at the temperature of the study. In this case, perhaps, the key role is played by the solubility of neodymium and cerium oxides in a molten $LiCl-Li_2O$ mixture. The X-ray diffraction patterns of the reduced samples presented in Figures 2 and 3 demonstrate the $LiNdO_2$ and $CeOCl$ phases. The presence of these substances is most likely associated with the occurrence of the following reactions in the melt [19,20]:

$$Ce_2O_{3(s)} + 2LiCl_{(l)} \rightarrow 2CeOCl_{(saturated)} + Li_2O_{(l)} \tag{3}$$

$$Nd_2O_{3(s)} + Li_2O_{(chloride\ melts)} \rightarrow 2LiNdO_{2(saturated).} \tag{4}$$

The presence of melt-soluble oxide and oxychloride forms of REM compounds provides neodymium and cerium access to the palladium surface, where the lithium concentration corresponds to the electrode potential. In addition, dissolved lithium is present in the salt electrolyte [21], which, due to the high porosity of the pellets, impregnates them well. Thus, at the surface of palladium grains, there are ionic forms containing neodymium or cerium, an alkali metal dissolved in the melt (and in palladium), and, of course, metallic palladium. The aforesaid factors create conditions for the reduction reaction of trivalent neodymium and cerium with lithium with the formation of intermetallic compounds of lanthanide and palladium:

$$CeOCl_{(saturate)} + 3Li_{(chloride\ melts,\ Pd)} + 3Pd_{(s)} \rightarrow CePd_{3(s)} + Li_2O_{(chloride\ melts)} + LiCl_{(l)} \tag{5}$$

$$LiNdO_{2(saturate)} + 3Li_{(chloride\ melts,\ Pd)} + 3Pd_{(s)} \rightarrow NdPd_{3(s)} + 2Li_2O_{(chloride\ melts)}. \quad (6)$$

It is important to note that in this case, the low solubility of REM oxide and oxychloride compounds [22] is compensated by very small distances between the reaction components in the reduced object pelletized at high pressure, which ensure quite sufficient rates of the corresponding reactions.

To confirm the mechanism of REM oxides reduction at positive potentials, a special experiment was carried out on the electrochemical reduction of a neodymium oxide pellet in contact with a palladium tablet. Figure 6 illustrates the pellets composed of Pd and Nd_2O_3, cathode design, and the cathode cross section after the electrolytic reduction.
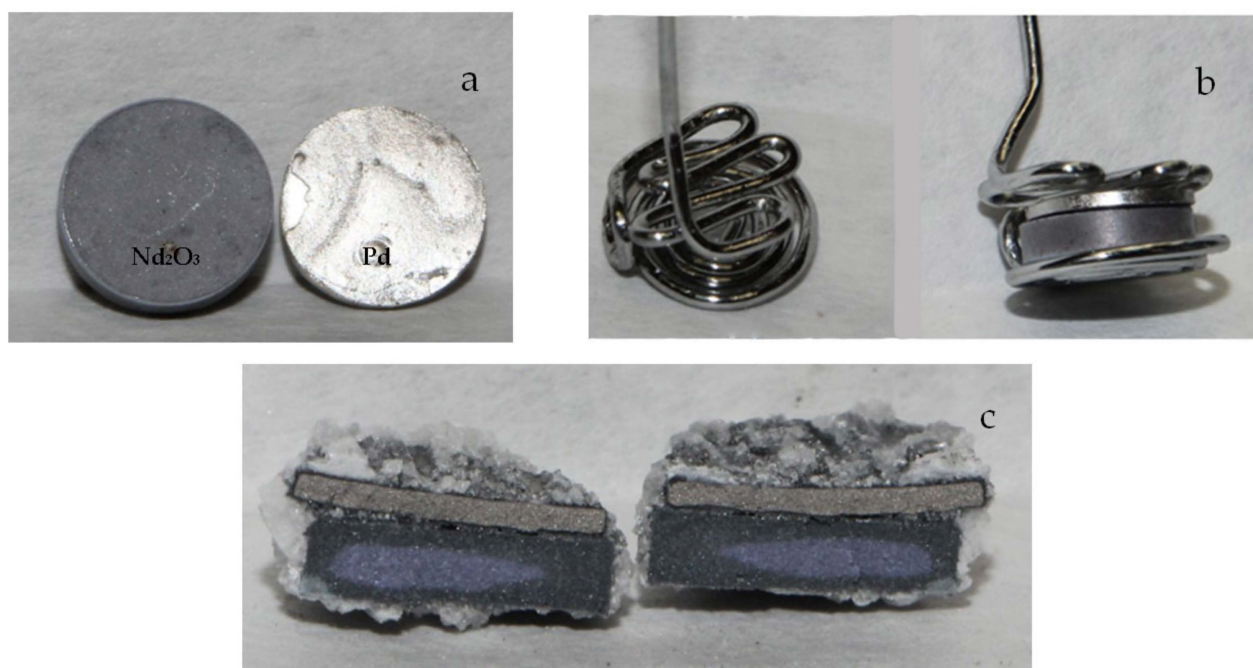

Figure 6. Appearance of Pd and Nd_2O_3 pellets before (**a**) and after (**c**) the experiment and a molybdenum current lead for clamping pelleted samples (**b**).

The experiment was carried out at a potential more positive than that of liquid lithium by ~0.7 V and 68% of the theoretically necessary electric current for the complete reduction of neodymium oxide to metal. After the electrolysis termination, the cathode was lifted from the melt, kept above the electrolyte surface to drain the trapped melt, and removed from the electrolytic cell. Figure 6c illustrates the cross section of the aggregated pellets with the electrolyte frozen at the outer surface. Figure 7 demonstrates a sample fragment rinsed in absolute ethanol. After rinsing in ethanol, various parts of the sample were examined using a Phenom ProX electron microscope (Phenom World BV, Eindhoven, the Netherlands) and a Rigaku 600 X-ray diffractometer (Rigaku, Japan). In Figure 6a,b it is seen that the pellets before the experiment did not adhere tightly to each other in all places. After the experiment, these voids turned out to be filled with crystals (photos in Figure 7), the composition of which, determined by an electron microscope, corresponded to an alloy of neodymium and palladium with a composition of 20–30 at.% Nd and 80–70 at.% Pd. X-ray phase analysis confirmed the presence of the $NdPd_3$ phase (Figure 8).
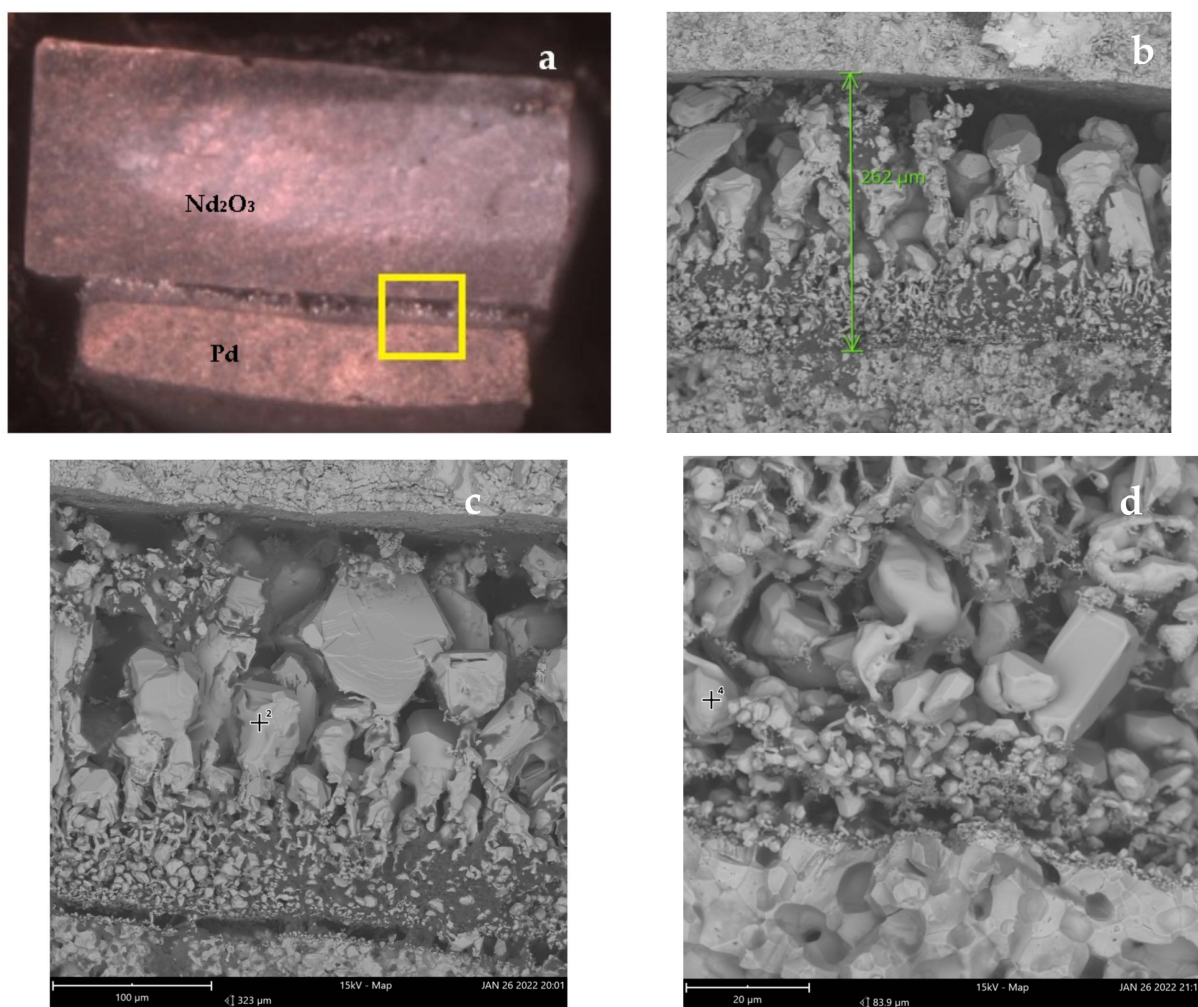
Figure 7. Photograph and SEM photographs of a fragment of Pd and Nd_2O_3 tablets rinsed after the experiment in ethanol. SEM images were made at different approximations using a Phenom Pro X electron microscope (Velmas Ltd., Saint Petersburg, Russia).
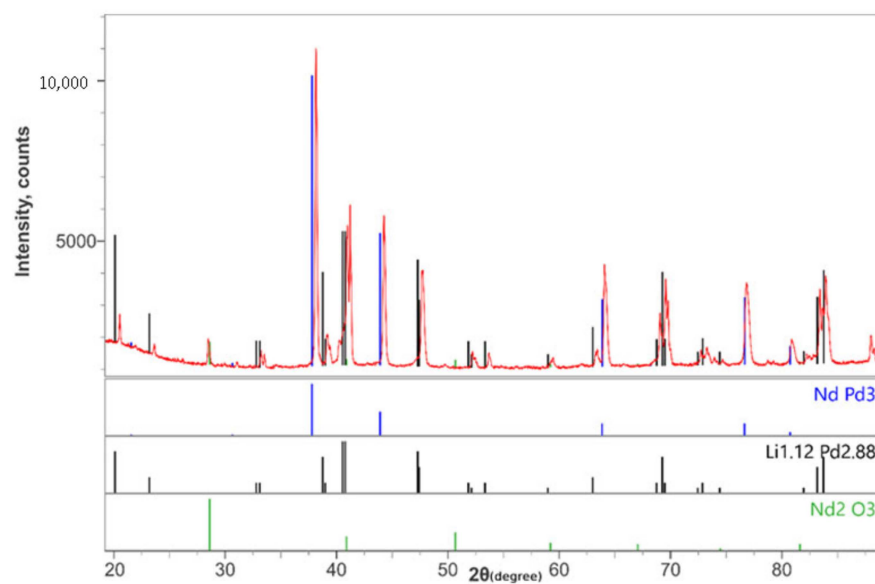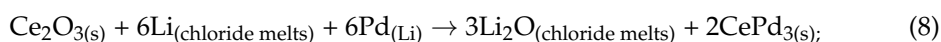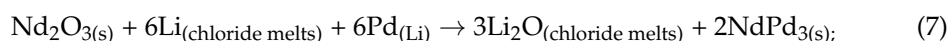

Figure 8. X-ray pattern of the surface of a palladium tablet after the experiment.

Figure 7 shows clearly that small intermetallic crystals begin to nucleate at the surface of the palladium pellet. Then, they grew towards the neodymium oxide pellet, increasing significantly in size, and finally reached the surface of the neodymium oxide pellet. The pellets were easily separated with a scalpel. Figure 8 shows the X-ray pattern of the surface area of the palladium pellet after separation. On a fragment of the surface of the neodymium oxide pellet, which was not in contact with the palladium pellet, only phases of neodymium oxide and lithium chloride were recorded.

The analysis of the experimental data of the reduced sample confirms the previously stated assumption that at positive potentials, the processes of neodymium oxide reduction and alloy formation begin at the surface of a palladium pellet, which, in fact, is an alloy of palladium and lithium containing an alkali metal corresponding to a potential of 0.7 V relative to $Li^+/Li°$, if we extrapolate the data of papers [15,16] to the temperature of 923 K. This is confirmed by the X-ray pattern presented in Figure 8. Further growth of crystals towards the neodymium oxide pellet is determined by the diffusion of palladium from its pellet, first into the bulk of the $NdPd_3$ intermetallic crystal and then to the surface, where further crystal growth occurs according to reaction (6). Lithium is delivered to the reaction zone from the salt melt since the solubility of the alkali metal in the Nd-Pd alloy is most likely insignificant.

The data available in the literature on the thermodynamics of Nd-Pd [23] and Ce-Pd [24] alloys make it possible to estimate the minimum value of lithium activity, and thus, the cathode potential, at which neodymium and cerium oxides can be reduced by lithium with the formation of an intermetallic compound of a certain composition. The calculations were carried out based on the reaction equations:

$$Nd_2O_{3(s)} + 6Li_{(chloride\ melts)} + 6Pd_{(Li)} \rightarrow 3Li_2O_{(chloride\ melts)} + 2NdPd_{3(s)};\qquad(7)$$

$$Ce_2O_{3(s)} + 6Li_{(chloride\ melts)} + 6Pd_{(Li)} \rightarrow 3Li_2O_{(chloride\ melts)} + 2CePd_{3(s)};\qquad(8)$$

$$\Delta G_{(reaction)} = 2\Delta G_{f(NdPd3)} + 3\Delta G_{f(Li2O)} - \Delta G_{f(Nd2O3)};$$

$$\Delta G_{(reaction)} = -RTlnK_{(reaction)}, K = (a_{Li2O})^3/[(a_{Li})^6 {}_* (a_{Pd})^6;$$

$$\Delta E = -(RT/F) \times ln(a_{Li})^6,$$

where:

$\Delta G_{f(Nd2O3)}$ is the change in the Gibbs energy of the neodymium oxide formation reaction at 923 K [25];

$\Delta G_{f(NdPd3)}$ is the change in the Gibbs energy of the reaction of the formation of $NdPd_3$ and $CePd_3$ intermetallic compounds at 923 K [23,24];

$\Delta G_{f(Li2O)}$ is the change in the Gibbs energy of the reaction of the formation of liquid lithium oxide at 923 K [25,26];

a_{Li2O} is the activity of lithium oxide in the chloride melt, calculated according to the scheme described in the work [26];
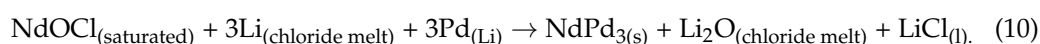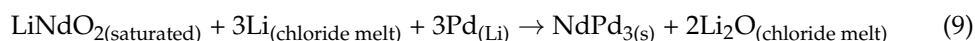
a_{Pd} is the activity of palladium in the Pd_7Li–Pd_2Li region according to the data reported in [15] extrapolated to the temperature of 923 K.

The calculation results are presented in Table 3.

Table 3. Cathode potentials (relative to $Li^+/Li°$), at which the reduction of neodymium and cerium oxides can begin with the formation of $NdPd_3$ and $CePd_3$ intermetallic compounds with palladium according to reactions (7), (8), (9), and (10) in the LiCl melt Li_2O(1.5 wt%).

Nd	E,V Reaction (7)	E,V Reaction (9)	E,V Reaction (10)	Ce Reaction (8)	E,V
$NdPd_3$	0.827	0.873	0.959	$CePd_3$	0.710

Considering that the reduction reaction of cerium and neodymium oxides proceeds with the participation of soluble forms of oxychlorides according to reaction (3), or double oxides according to reaction (4),

$$LiNdO_{2(saturated)} + 3Li_{(chloride\ melt)} + 3Pd_{(Li)} \rightarrow NdPd_{3(s)} + 2Li_2O_{(chloride\ melt)} \quad (9)$$

$$NdOCl_{(saturated)} + 3Li_{(chloride\ melt)} + 3Pd_{(Li)} \rightarrow NdPd_{3(s)} + Li_2O_{(chloride\ melt)} + LiCl_{(l)}. \quad (10)$$

Taking into account the thermodynamic data on the formation of the necessary neodymium compounds [19,25], the values of potentials, at which the reduction process initiates according to reactions (9) and (10), are provided in Table 3. The performed calculations confirm the possibility of reducing pelleted powder mixtures of neodymium and cerium oxides with palladium at positive cathode potentials with the formation of $LnPd_3$ intermetallic compounds.

5. Conclusions

The electrochemical reduction of the CeO_2-Pd, Nd_2O_3-Pd, and CeO_2-Pd-Nd_2O_3 pellets in a lithium chloride melt with small additions of lithium oxide at a temperature of 923 K has been studied. It is shown that in a wide range of cathode potentials, the reduction of lanthanide oxides occurs with the formation of intermetallic compounds with palladium. Using X-ray diffraction of the reduced samples, it was found that in the range of cathode potentials ~0.8 V relative to Li^+/Li^0, the intermetallic compounds of the $CePd_3$ and $NdPd_3$ compositions were formed. The shift of the potentials to a region close to the potential of the alkali metal liquid phase formation relative to Li^+/Li^0 at the cathode leads to the formation of intermetallic compounds with higher REM concentrations: CePd, NdPd, Ce_3P_4, and Nd_3Pd_4. The degree of REM oxides reduction and the composition of the resulting alloys were calculated based on the residual oxygen concentration in the reduced samples. The calculations carried out on the basis of the thermodynamic parameters available in the literature for intermetallic compounds of cerium and neodymium with palladium are in good agreement with the obtained experimental data. Possible mechanisms of the alloy formation are considered and analyzed. The solubility of lanthanide oxides in a salt melt and the formation of a lithium–palladium liquid alloy are extremely important for the formation of intermetallic compounds.

Author Contributions: Conceptualization, V.Y.S. and Y.P.Z.; methodology, V.Y.S. and A.B.S.; validation, V.Y.S. and A.B.S.; formal analysis, A.A.M.; investigation, A.V.S. and P.N.M.; resources, A.A.M.; data curation, A.V.S. and P.N.M.; writing—original draft preparation, V.Y.S.; writing—review and editing, V.Y.S.; visualization, A.V.S.; supervision, Y.P.Z.; project administration, Y.P.Z. All authors have read and agreed to the published version of the manuscript.

References

1. Imoto, S. Chemical state of fission products in irradiated UO$_2$. *J. Nucl. Mater.* **1986**, *140*, 19–27. [CrossRef]
2. Bush, R.P. Recovery of platinum group metals from high level radioactive waste. *Platin. Met. Rev.* **1991**, *35*, 202–208.
3. Shishkin, A.V.; Shishkin, V.Y.; Salyulev, A.B.; Kesikopulos, V.A.; Kholkina, A.S.; Zailov, Y.P. Electrochemical reduction of uraniumdioxide in LiCl-Li2O melt. *At. Energy* **2021**, *131*, 77–82. [CrossRef]
4. Shishkin, A.V.; Shishkin, V.Y.; Pankratov, A.A.; Burdina, A.A.; Zaikov, Y.P. Electrochemical Reduction of La2O3, Nd2O3, and CeO2 in LiCl-Li2O Melt. *Materials* **2022**, *15*, 3963. [CrossRef]
5. Okamoto, H. Nd-Pd (neodymium-palladium). *J. Phase Equilibria Diffus.* **1992**, *13*, 220–222. [CrossRef]
6. Okamoto, H. Ce-Pd (cerium-palladium). *J. Phase Equilibria Diffus.* **1991**, *12*, 700–701. [CrossRef]
7. Palenzona, A.; Canepa, F. The phase diagrams of the La-Ru and Nd-Ru systems. *J. Less Common Met.* **1990**, *157*, 307–313. [CrossRef]
8. Palenzona, A. The phase diagram of the Ce-Ru system. *J. Alloys Compd.* **1991**, *176*, 241–246. [CrossRef]
9. Laidler, J.J.; Battles, J.E.; Miller, W.E.; Ackerman, J.P.; Carls, E.L. Development of pyroprocessing technology. *Prog. Nucl. Energy* **1997**, *31*, 131–140. [CrossRef]
10. Ackerman, J.P. Chemical basis for pyrochemical reprocessing of nuclear fuel. *Ind. Eng. Chem. Res.* **1991**, *30*, 141–145. [CrossRef]
11. Nikolaev, A.Y.; Mullabaev, A.R.; Suzdaltsev, A.V.; Kovrov, V.A.; Kholkina, A.S.; Shishkin, V.Y.; Zaikov, Y.P. Purification of Alkali-Metal Chlorides by Zone Recrystallization for Use in Pyrochemical Processing of Spent Nuclear Fuel. *At. Energy* **2022**, *131*, 195–201. [CrossRef]
12. Shishkin, V.Y.; Mityaev, V.S. Alkali halides purification by zone melting (Ochistka galoguenidov shelochnykh metallov motodom zonnoy plavki). *Izv. ANSSSR Inorg. Mater.* **1982**, *11*, 1917–1918.
13. Salyulev, A.B.; Shishkin, A.V.; Shishkin, V.Y.; Zaikov, Y.P. Distillation of lithium chloride from the products of uranium dioxide metallization. *At. Energy* **2019**, *126*, 226–229. [CrossRef]
14. Rossi, D.; Ferro, R.; Marazza, R. X-ray diffraction data of palladium-rich cerium-palladium alloys. *J. Less Common Met.* **1975**, *40*, 345–350. [CrossRef]
15. Nohira, T.; Ito, Y. Thermodynamic Properties of Pd-Li Alloys. *J. Electrochem. Soc.* **1998**, *145*, 785. [CrossRef]
16. Nohira, T.; Amezawa, K.; Ito, Y. Electrochemical formation of Pd-Li alloys in LiCl-KCl eutectic melts. *J. Appl. Electroch.* **1995**, *25*, 48–53. [CrossRef]
17. Kim, D.-H.; Kim, J.-Y.; Park, Y.J.; Bae, S.-Y.; Park, T.H.; Song, K. Solubility measurement of Li$_2$O in LiCl molten salt for electro-reduction process. *Asian J. Chem.* **2013**, *25*, 7055. [CrossRef]
18. Tsuyoshi, U.; Kurata, M.; Inoue, T.; Sims, H.E.; Beetham, S.A.; Jenkins, J.A. Pyrochemical reduction of uranium dioxide and plutonium dioxide by lithium metal. *J. Nucl. Mater.* **2002**, *300*, 15–26.
19. Gourishankar, K.V.; Johnson, G.K.; Johnson, I. Thermodynamics of mixed oxide compounds, Li$_2$O● Ln$_2$O$_3$ (Ln= Nd or Ce). *Met. Mater. Trans. B* **1997**, *28*, 1103–1110. [CrossRef]
20. Hur, J.M.; Kim, T.J.; Choi, I.K.; Do, J.B.; Hong, S.S.; Seo, C.S. Chemical behavior of fission products in the pyrochemical process. *Nucl. Technol.* **2008**, *162*, 192–198. [CrossRef]
21. Tsuyoshi, N.; Ryohei, M.; Koichiro, N.; Nobuatsu, W. Miscibility of lithium with lithium chloride and lithium chloride–potassium chloride eutectic mixture. *Bull. Chem. Soc. Jpn.* **1974**, *47*, 2071–2072.
22. Kato, T.; Sakamura, Y.; Iwai, T.; Arai, Y. Solubility of Pu and rare-earths in LiCl-Li$_2$O melt. *Radiochim. Acta* **2009**, *97*, 183–186. [CrossRef]
23. Hennemann, K.; Schaller, H.J. Thermodynamic Properties of Pd-Nd Alloys. *Ber. Bunsenges. Phys. Chem.* **1995**, *99*, 1015–1019. [CrossRef]
24. Bretschneider, T.; Schaller, H.-J. A Thermodynamic Study of Pd—Ce Alloys Using CeF3 as Electrolyte. *Ber. Bunsenges. Phys. Chem.* **1990**, *94*, 185–190. [CrossRef]
25. HSC Roine, A. HSC Chemistry® (Software). Outotec: Pori, Finland. 2018. Available online: www.outotec.com/HSC (accessed on 18 April 2022).
26. Usami, T.; Kato, T.; Kurata, M.; Inoue, T.; Sims, H.E.; Beetham, S.A.; Jenkins, J.A. Lithium reduction of americium dioxide to generate americium metal. *J. Nucl. Mater.* **2002**, *304*, 50–55. [CrossRef]